TITLE PAGE

The Central Nervous System Modulates the Neuromechanical Delay in a Broad Range for the Control of Muscle Force

A. Del Vecchio[1,5], A. Úbeda[2], M. Sartori[3], JM Azorín[4], F. Felici[5], D. Farina[1]

Abbreviated title: Introducing the Neuromechanical Delay

Affiliations

[1]Department of Bioengineering, Imperial College London, SW7 2AZ, London, UK.

[2]Department of Physics, Systems Engineering and Signal Theory, University of Alicante, 03690, Spain.

[3]Institute of Biomedical Technology and Technical Medicine, Department of Biomechanical Engineering, University of Twente, 7522 NB, Enschede, The Netherlands.

[4]Systems Engineering and Automation Department BMI Systems Lab, University Miguel Hernández of Elche, 03202, Spain.

[5]Department of Movement, Human and Health Sciences, University of Rome "Foro Italico", 00135 Rome, Italy.

Corresponding author:

D. Farina. Department of Bioengineering, Imperial College London, SW7 2AZ, London, UK. Tel: Tel: +44 (0)20 759 41387, Email: d.farina@imperial.ac.uk

Keywords:

Electromechanical delay; Neural Drive; Motor unit; Force Prediction; Sinusoidal Contractions;

ABSTRACT

Force is generated by muscle units according to the neural activation sent by motor neurons. The motor unit is therefore the interface between the neural coding of movement and the musculotendinous system. Here we propose a method to accurately measure the latency between an estimate of the neural drive to muscle and force. Further, we systematically investigate this latency, that we refer to as the neuromechanical delay (NMD), as a function of the rate of force generation. In two experimental sessions, eight men performed isometric finger abduction and ankle dorsiflexion sinusoidal contractions at three frequencies and peak-to-peak amplitudes [0.5,1,1.5 (Hz); 1,5,10 of maximal force (%MVC)], with a mean force of 10% MVC. The discharge timings of motor units of the first dorsal interosseous (FDI) and tibialis anterior (TA) muscle were identified by high-density surface EMG decomposition. The neural drive was estimated as the cumulative discharge timings of the identified motor units. The neural drive predicted 80 ± 0.4% of the force fluctuations and consistently anticipated force by 194.6 ± 55 ms (average across conditions and muscles). The NMD decreased non-linearly with the rate of force generation (R^2 = 0.82 ± 0.07; exponential fitting) with a broad range of values (from 70 to 385 ms) and was 66 ± 0.01 ms shorter for the FDI than TA ($P<0.001$). In conclusion, we provided a method to estimate the delay between the neural control and force generation and we showed that this delay is muscle-dependent and is modulated within a wide range by the central nervous system.

New & Noteworthy

The motor unit is a neuromechanical interface that converts neural signals into mechanical force with a delay determined by neural and peripheral properties. Classically, this delay has been assessed from the muscle resting level or during electrically elicited contractions. In the present study we introduce the neuromechanical delay as the latency between the neural drive to muscle and force during variable-force contractions, and we show that it is broadly modulated by the central nervous system.

INTRODUCTION

Movement is the result of the interaction between neural and muscular structures. Neuromechanics aims at understanding the functional effects of the neural coding of movement. The motor unit is the interface between neural coding (by motor neurons) and force generation (by muscle units). The conversion of neural code to force has a latency due to the dynamic sensitivity of the motor neurons (1) and to the time needed to stretch the series elastic components (SEC) of the muscle-tendon unit following the depolarization of the muscle fibers (19, 22).

Estimates of the electromechanical delay (EMD) have been obtained during voluntary and electrically-elicited contractions (18, 25, 29, 30) or in isolated animal preparations (1). However, these methods do not provide information on the delay between neural drive to muscles and force during contractions with force modulation since they are obtained from the muscle resting state or during electrically-induced contractions (1, 4, 19, 22, 28). Moreover, with these approaches it is not possible to investigate the potential task-dependent changes of EMD. Indeed, it is generally believed that the EMD is a constant property of a muscle (19, 22).

The estimates of EMD are significantly greater when they are obtained during voluntary force generation than electrically-elicited contractions (25, 30). This indicates that the EMD depends on the properties of the recruited motor units. Since the motor unit twitch properties vary widely within a muscle (5, 17), we hypothesized that the delay between neural drive to muscle and force varies within a large range of values during voluntary tasks. Because of technical limitations, an estimate of the delay between neural drive to muscle and force across conditions has not been previously possible.

Here we define the neuromechanical delay (NMD) as the latency between the neural drive to muscle and force during voluntary contractions of variable force and we propose an accurate methodology for its estimation across a broad range of conditions. Further, we test the hypothesis that the central nervous system (CNS) modulates the NMD in a wide range of values. The results provide evidence of a functional tuning of the NMD by the CNS.

METHODS

Eight moderately active men participated to the experiments (age 27.2 ± 2.2 year; body mass 79.5 ± 2.5 kg; height 178.4 ± 6.5 cm). The experiments were approved by the Ethical Committee of the Universitätsmedizin Göttingen, approval n. (1/10/12). Before taking part in the testing measurements an informed written consent was signed by all subjects. None of the subjects reported any history of neuromuscular disorders or upper limb pathology or surgery.

Experimental Design

Experiments for the upper and lower limb were performed in two days separated by one week. In each experiment, the participants performed three isometric index finger-abduction maximal voluntary contractions (MVC) or three isometric ankle-dorsiflexion MVC with their dominant limb (self-reported) and nine trials of isometric sinusoidal force contractions at different amplitudes and frequencies. The joint force signal was visualized on a monitor positioned directly in front of the subjects. The MVC feedback and sine wave trajectories were displayed through a custom MATLAB script (MathWorks, Inc., Natick, Massachusetts, USA). During the MVC, the participants were verbally encouraged to 'push as hard as possible' for at least 3 s. The maximal MVC value was recorded and used as a reference value for the sinusoidal isometric contractions. Participants were asked to track sinusoidal force trajectories at the frequencies 0.5, 1, or 1.5 Hz and amplitudes 1, 5, or 10% MVC, in all combinations (9 tasks in total), for 2 min. The mean level of the target trajectories was 10% MVC. The 9 tasks were performed in a random order with a recovery time of 3 min between tasks.

Force and EMG recordings

For the finger abduction experiments, participants comfortably seated with the dominant arm (self-reported) placed in a custom-made isometric dynamometer that immobilized the forearm and restrained the wrist and fingers. Isometric force during finger abduction was measured by a strain gauge that was positioned perpendicular to the index finger. This setup allowed recording the force directly arising from the abduction of the finger. For the ankle dorsiflexion measurements, participants were seated in an isometric dynamometer Biodex System 3 (Biodex Medical System Inc., Shirley, NY, USA) in an upright position, with the dominant leg (self-reported) extended and the ankle flexed at 30° with respect to neutral position. The ankle joint and the foot were fastened with Velcro straps. High-density surface electromyography (HDsEMG) signals were recorded from the first dorsal interosseous muscle (FDI) or the tibialis anterior muscle (TA) in each session by using a grid of 64 electrodes (5 columns, 13 rows; gold-coated; 2-mm diameter (FDI), 4-mm diameter (TA); interelectrode distance: 4 mm (FDI), 8 mm (TA); OT Bioelettronica, Torino, Italy). Before placing the

HDsEMG grid, the skin was shaved, lightly abraded and cleansed with 70% ethanol. The electrode grid was placed on the skin with a conductive paste (SpesMedica, Battipaglia, Italy) that established the skin-electrode contact. HDsEMG signals were recorded in monopolar derivation (3-dB bandwidth 10-500 Hz; EMG-USB2+ multi-channel amplifier, OT Bioelettronica, Torino, Italy) and digitally converted on 12 bits at 2048 samples/s. The EMG and joint torque were concurrently recorded by the same acquisition system.

High-density EMG decomposition

The HDsEMG signals were digitally filtered with a band-pass filter at 20-500 Hz (2^{nd} order, Butterworth). Then they were decomposed into the activity of individual motor units with an extensively validated decomposition algorithm (13, 15, 21, 26). Motor units with a pulse-to-noise ratio (14) less than 30 dB and/or with discharges separated by more than 2 s were discarded from further analysis. The individual motor unit discharge timings were summed to generate a cumulative spike train (CST). The CST is an estimate of the neural drive sent to the muscle (9, 20). Since the number of discharges per second in the CST depends on the number of decomposed motor units, we further calculated the average number of discharges per motor unit per second, as the number of discharges in the CST per second divided by the number of decomposed motor units (DR, s^{-1}).

NMD estimation

We defined the NMD as the time delay between the rise time of the motor unit action potentials and the respective force output identified by the cross-correlogram. For the computation of the delay between neural drive and force, a band-pass filter (bandwidth 2 Hz) was applied to the CSTs and force signals (4th order zero-phase Butterworth filter). After filtering, the CST and force signals were divided into one-cycle time frames and the cross-correlation between CST and force was computed for each time frame and then averaged across all time frames. The time lag of the peak of the cross-correlation function provided an estimate of the NMD. The estimated NMD was associated to frequency and amplitude of the sinusoidal contractions as well as to the maximum rate of change of force, i.e. the first derivative of force (proportional to the product of amplitude and frequency). Finally, the force and trajectory profiles were cross-correlated to assess the force tracking accuracy.

Statistical Analysis

A three-way (2 muscles x 3 frequencies x 3 force levels) repeated measures ANOVA was computed for the NMD and the estimated force accuracy. When an interaction as found, a Bonferroni correction was applied

to account for multiple comparisons. Finally, linear and non-linear regression was used to fit the values of NMD and DR as a function of the force derivative. Data are reported as mean ± SD. The significance level was set to $P < 0.05$.

RESULTS

High-density EMG decomposition

The total number of decomposed motor units for all subjects and conditions was 1170 for the FDI and 3357 for the TA muscle. The average number of identified motor units for each subject and condition was 8.66 ± 3.27 and 21.3 ± 5.34 for the FDI and TA, respectively.

Neuromechanical delay

There was no difference in the force tracking accuracy between muscles (R=0.68 ± 22.67 and R=0.68 ± 21.09, for FDI and TA; P>0.05). However, the increase in frequency determined a decrease in the tracking accuracy for both the FDI and TA muscle (R= 85.9 ± 7.14, 79.5 ± 4.69, 41.3 ± 4.33 for FDI, and R= 85.6 ± 8.45, 77.2 ± 5.05, 41.3 ± 3.84, for TA, for 0.5, 1, and 1.5 Hz, respectively).

Figure 1 shows a representative example of estimation of NMD. At the group level, the filtered CST predicted 83 ± 0.20% and 76 ± 0.14% of the force fluctuations for the FDI and TA muscle, respectively. The latency between the CST and force ranged from 70 ms to 334 ms for the FDI and from 138 ms to 385 ms for the TA, depending on the task. The NMD was significantly smaller for the FDI than the TA muscle [average across conditions, 164.5 ± 60 ms vs. 224.7 ± 50 (ms), ANOVA, P<0.001].

Figure 2 shows the average latency for all subjects at each target amplitude and frequency of the sinusoid. The increase in either frequency or amplitude determined a decrease in the NMD (ANOVA p<0.001). The NMD values were consistently greater during the low-force slow-oscillation tasks than for larger and faster oscillations. The shortest NMD corresponded to the highest target frequency and peak-to-peak amplitude (1.5 Hz; 10 %MVC). At the same relative target amplitudes, the change in the frequency of the sine wave decreased the NMD significantly (Fig. 2). An example is represented in Figure 1 that shows that at the same relative peak-to-peak amplitude of 5% (MVC), a change in frequency from 0.5 Hz to 1 Hz determined a decrease in NMD by approximately 50 ms. These results were confirmed by the group analysis (Figure 2). For example, when the peak-to-peak amplitude of the sine wave was 1% MVC, the NMD decreased significantly as a function of frequency, with a mean difference of 134.4 ± 33.5 (ms) and 143.6 ± 16.2 (ms)

between 0.5 and 1.5 Hz, for the FDI and TA muscle respectively. This indicated that the NMD varied widely when generating the same forces at different rates of force generation.

Overall, the NMD in the two muscles changed as a function of both frequency and amplitude. The analysis of the force derivative (slope) (Fig. 3) indicated a strong association of the NMD with the product of frequency and amplitude (i.e., speed of the contraction). The NMD decreased in a non-linear way with an increase in contraction speed (Fig. 3).

Discharge rate

The average motor unit discharge rate ranged from 1.18 to 17.66 pps (FDI) and from 1.03 to 12.22 pps (TA), with average values across all conditions of 9.06 ± 4.15 pps (FDI) and 8.50 ± 2.62 pps (TA). The average motor unit discharge rate was negatively associated to the rate of change of force (R^2 = 0.95 ($p<0.001$) and R^2 = 0.75 ($p<0.01$) for the FDI and TA respectively). This negative association indicates a decrease in the average number of discharges per motor unit with an increase in speed of the contraction.

DISCUSSION

We have defined the NMD as the time difference between the neural command to muscle and the generated force during voluntary tasks. An estimate of the NMD can be obtained from the time lag of the peak of the cross-correlation between an estimate of the neural drive and force. The estimated NMD was on average ~200 ms and was modulated by the CNS according to the contraction speed. The NMD is intrinsically related to the motor unit twitch properties and can thus be modulated following the size principle.

Estimate of the neuromechanical delay

For both muscles, the correlation between the estimated neural drive and force was on average >75%, indicating accurate EMG decomposition over relatively large motor unit populations and robust delay estimation. Conversely, previous studies that cross-correlated individual motor unit discharge timings with force during sinusoidal contractions reported values of correlation <10% (7). The high correlation values in this study allowed us to define a robust estimate of the delay whereas the mathematical definition of a delay does not hold for low correlation values (since two signals of different shape cannot be seen as delayed version of each other). Since the CST represents common input components shared between motor neurons (8), the identification of a relatively large number of motor units improved the prediction of force fluctuations and the accuracy in delay estimates (20).

Factors determining the NMD

The motor unit recruitment pattern is related to the biophysical properties of the motor neurons. Motor unit properties vary widely in a muscle and depend on the recruitment threshold of the motor neuron (2, 5, 12, 26, 27). The wide distribution of properties of motor units in an individual muscle explains the possibility of modulating the NMD.

Because the NMD depends on the dynamic sensitivity of the motor neurons (1) and the intrinsic properties of the musculotendinous system, the CNS can modulate the NMD only by varying the activation of muscle units. This activation is constrained in order by the size principle (11). However, the motor unit recruitment thresholds depend on the rate of force development (6, 24). Therefore, the NMD can be modulated by tuning the recruitment thresholds, maintaining the ordering by size. The recruitment of motor neurons depends on the net excitatory input they receive (10). The need for generating faster contractions determines a decrease in recruitment threshold so that a greater number of motor units is recruited for the same force. This compressed recruitment range is compensated by a decrease in the average discharge rate per motor unit, as shown in Fig. 4. The underpinning mechanisms determining a decrease in the NMD with frequency and/or amplitude of the sinusoid thus differ. The amplitude of sinusoidal force contractions is increased by recruitment and increased discharge rate while the frequency is increased by a compressed recruitment and a decrease in average discharge.

The association between motor unit twitch properties and NMD is also confirmed by the differences found between FDI and TA. The full motor unit recruitment for the FDI and TA muscle differs. The FDI motor units are fully recruited at ~50% MVC (16), whereas the pool of motor units innervating the TA muscle completes recruitment at ~90% MVC (5). Thus, at the same relative force, the FDI recruits relatively larger motor units (with faster twitches) compared to the TA. Although previous evidence from individual motor unit measures of twitch tension and contraction times indicate relatively similar mechanical properties for these two muscles (3, 5), the muscle fiber composition and tendon stiffness may also contribute to the differences in NMD. In animal preparations, when stimulating motor neurons with sine waves, the delay between stimulation and force (equivalent to our NMD) decreases with increasing stimulation frequency due to the dynamic sensitivity of the motor neurons (1). Moreover, the slow twitch motor units tend to have a shorter NMD when compared to the fast ones (1). Indeed, sine-wave stimulations of cat soleus axons shows a smaller NMD when compared to the gastrocnemius muscle due to slower rise time of soleus motor unit twitches (23).

The proposed approach provides a precise analysis of the delay that the CNS experiences in providing neural command to the muscles during force modulation in humans. This analysis allows the establishment of a functional link between the neural and muscular mechanisms of force generation. The decrease in NMD with the rate of force generation presumably serves the functional purpose of optimising the force control accuracy. The tracking accuracy decreased with an increase in the frequency of the sine-wave in this study but the decrease was relatively limited, likely due to a shorter control delay. A shorter delay between neural command and force generation indeed implies a larger bandwidth of control, extending the functional range of accurate motor tasks to faster movements. This may be specifically relevant for hand muscles that require precise control for fast and dexterous hand tasks. Indeed, our results showed a large difference in NMD between a hand and a leg muscle. From the functional view, the time delay that the CNS experiences between neural commands and force generation continuously changes over time during natural tasks, according to the instantaneous changes in speed of the task. This variation is not determined by a direct modulation but is the result of the distribution of muscle unit properties and of the intrinsic properties of motor neurons. This tuning presumably allows optimal control over a large range of conditions without any cognitive effort. Nonetheless, despite the smaller NMD observed for the FDI muscle, we did not detect any differences in the tracking accuracy between the two muscles. This contradictory observation should be analysed in further studies.

Neuromechanical and electromechanical delay

The defined NMD is very different from the classic EMD. Indeed, the NMD is the delay between neural drive and force during tasks with any rate of force variations while the EMD is measured from the interference EMG (“electro”, not “neuro”) at the instant of sudden force changes (e.g., during ballistic or electrically elicited contractions). Classic EMD values are considerably shorter when compared to our results on NMD. EMD estimates are obtained as the time difference between the onset of the surface EMG signal and the onset of force. During electrical stimulation, the EMD in the gastrocnemius muscle is only ~15 ms (19, 22). During voluntary contractions from the muscle resting state, the EMD is ~38 ms in the vastus lateralis (ms) (and ~17 ms in the same muscle during electrical stimulations) (30). The estimates of EMD were found slightly greater, although still smaller than the currently estimated NMD, for the biceps brachii muscle during voluntary fast contractions starting from a baseline level (~70 ms) (28). The reason for the different estimates of EMD with respect to our NMD are not only related to the use of the EMG but, mainly, to the type of contractions used for the estimate.

The NMD is influenced by the time to peak of the twitches of the active motor units that range widely within a muscle (e.g., 51 to 114 ms for the TA muscle (5)). Therefore, the active part of the SEC in single motor units significantly contributes to the NMD. This finding is in disagreement with previous examinations of the determinants of EMD during electrically induced contractions. These previous studies indicate that 52% of the EMD depends on the properties of the aponeurosis and the tendon (i.e., the non-active part of the SEC) (22), with the tendon slack contributing significantly to the EMD (19).The NMD in the present study was largely modulated by the CNS by recruitment of motor units rather than being influenced by the non-active part of the SEC. Indeed, at similar frequencies and peak-to-peak amplitudes of the sinusoidal forces as in the present study, the NMD was significantly smaller when compared to a continuous stretch of the muscle-tendon unit (1 %MVC, 1 Hz). Finally, sine wave stimulations of motor axons or individual motor neurons in animal studies also show large estimates of NMD, similar to the present study (1, 23).

Conclusion

We proposed a novel method to accurately estimate the delay between the neural code and the mechanics of muscle contraction during voluntary tasks, defined here as NMD. Previous studies determined an EMD during electrically-induced contractions or from a resting condition that provide results dissociated from the actions of the CNS during functional force modulation. The NMD ranged broadly and was associated to the rate of force development, so that faster contractions were performed with shorter NMD. These results indicate that the NMD is intrinsically related to the recruitment of motor units with a wide range of mechanical properties, so that it can be modulated broadly within the constraints of the size principle.

Conflict of interest

The authors declare no competing financial interests

Acknowledgments

This work was partly funded by the ERC Advanced grant DEMOVE (267888) and Proof-of-Concept Project Interspine (737570).

REFERENCES

1. **Baldissera F**, **Cavallari P**, **Cerri G**. Motoneuronal pre-compensation for the low-pass filter characteristics of muscle. A quantitative appraisal in cat muscle units. *J Physiol* 511: 611–627, 1998.

2. **Burke RE**. Motor units: anatomy, physiology, and functional organization. *Handb Physiol - Nerv Syst* 543: 345–422, 2011.

3. **Carpentier A**, **Duchateau J**, **Hainaut K**. Motor unit behaviour and contractile changes during fatigue in the human first dorsal interosseus. *J Physiol* 534: 903–912, 2001.

4. **Cavanagh PR**, **Komi P V.** Electromechanical delay in human skeletal muscle under concentric and eccentric contractions. *Eur J Appl Physiol Occup Physiol* 42: 159–163, 1979.

5. **Van Cutsem M**, **Feiereisen P**, **Duchateau J**, **Hainaut K**. Mechanical properties and behaviour of motor units in the tibialis anterior during voluntary contractions. *Can J Appl Physiol* 22: 585–597, 1997.

6. **Desmedt JE**, **Godaux E**. Ballistic contractions in man: characteristic recruitment pattern of single motor units of the tibialis anterior muscle. *J Physiol* 264: 673–693, 1977.

7. **Erimaki S**, **Agapaki OM**, **Christakos CN**. Neuromuscular mechanisms and neural strategies in the control of time-varying muscle contractions. *J Neurophysiol* 110: 1404–1414, 2013.

8. **Farina D**, **Negro F**. Common Synaptic Input to Motor Neurons, Motor Unit Synchronization, and Force Control. *Exerc Sport Sci Rev* 43: 23–33, 2015.

9. **Farina D**, **Negro F**, **Dideriksen JL**. The effective neural drive to muscles is the common synaptic input to motor neurons. *J Physiol* 49: 1–37, 2014.

10. **Gabriel JP**, **Ausborn J**, **Ampatzis K**, **Mahmood R**, **Eklöf-Ljunggren E**, **El Manira A**. Principles governing recruitment of motoneurons during swimming in zebrafish. *Nat Neurosci* 14: 93–99, 2011.

11. **Henneman E**. Relation between size of neurons and their susceptibility to discharge. *Science* 126: 1345–7, 1957.

12. **Henneman E**, **Somjen G**, **Carpenter DO**. Functional Significance of Cell Size in Spinal Motoneurons. *J Neurophysiol* 28: 560–580, 1965.

13. **Holobar A**, **Minetto M a**, **Farina D**. Accurate identification of motor unit discharge patterns from high-density surface EMG and validation with a novel signal-based performance metric. *J Neural Eng* 11:

016008, 2014.

14. **Holobar A**, **Minetto MA**, **Farina D**. Accurate identification of motor unit discharge patterns from high-density surface EMG and validation with a novel signal-based performance metric. *J Neural Eng* 11: 016008, 2014.

15. **Holobar A**, **Zazula D**. Multichannel blind source separation using convolution Kernel compensation. *IEEE Trans Signal Process* 55: 4487–4496, 2007.

16. **De Luca CJ**, **LeFever RS**, **McCue MP**, **Xenakis AP**. Behaviour of human motor units in different muscles during linearly varying contractions. *J Physiol* 329: 113–128, 1982.

17. **McNulty P a**, **Falland KJ**, **Macefield VG**. Comparison of contractile properties of single motor units in human intrinsic and extrinsic finger muscles. *J Physiol* 526 Pt 2: 445–456, 2000.

18. **Minshull C**, **Gleeson N**, **Walters-Edwards M**, **Eston R**, **Rees D**. Effects of acute fatigue on the volitional and magnetically-evoked electromechanical delay of the knee flexors in males and females. *Eur J Appl Physiol* 100: 469–478, 2007.

19. **Muraoka T**, **Muramatsu T**, **Fukunaga T**, **Kanehisa H**. Influence of tendon slack on electromechanical delay in the human medial gastrocnemius in vivo. *J Appl Physiol* 96: 540–544, 2004.

20. **Negro F**, **Holobar A**, **Farina D**. Fluctuations in isometric muscle force can be described by one linear projection of low-frequency components of motor unit discharge rates. *J Physiol* 587: 5925–5938, 2009.

21. **Negro F**, **Muceli S**, **Castronovo AM**, **Holobar A**, **Farina D**. Multi-channel intramuscular and surface EMG decomposition by convolutive blind source separation. *J Neural Eng* 13: 026027, 2016.

22. **Nordez A**, **Gallot T**, **Catheline S**, **Guével A**, **Cornu C**, **Hug F**. Electromechanical delay revisited using very high frame rate ultrasound. *J Appl Physiol* 106: 1970–1975, 2009.

23. **Partridge LD**. Modifications of neural output signals by muscles: a frequency response study. *J Appl Physiol* 20: 150–156, 1965.

24. **Rome LC**, **Funke RP**, **Alexander RM**, **Lutz G**, **Aldridge H**, **Scott F**, **Freadman M**. Why animals have different muscle fibre types. *Nature* 335: 824–827, 1988.

25. **Tillin NA**, **Jimenez-Reyes P**, **Pain MTG**, **Folland JP**. Neuromuscular performance of explosive power athletes versus untrained individuals. *Med Sci Sports Exerc* 42: 781–790, 2010.

26. **Del Vecchio A**, **Negro F**, **Felici F**, **Farina D**. Distribution of muscle fiber conduction velocity for representative samples of motor units in the full recruitment range of the tibialis anterior muscle. *Acta Physiol Scand* 38: 42–49, 2017.

27. **Del Vecchio A**, **Negro F**, **Felici F**, **Farina D**. Associations between motor unit action potential parameters and surface EMG features. *J Appl Physiol* 123: 835–843, 2017.

28. **Vint PF**, **McLean SP**, **Harron GM**. Electromechanical delay in isometric actions initiated from nonresting levels. *Med Sci Sports Exerc* 33: 978–983, 2001.

29. **Zhou S**. Acute effects of repeated maximal isometric contraction on electromechanicsl delay of knee extensor muscle. *J Electromyogr Kinesiol* 6: 117–127, 1996.

30. **Zhou S**, **Lawson DL**, **Morrison WE**, **Fairweather I**. Electromechanical delay in isometric muscle contractions evoked by voluntary, reflex and electrical stimulation. *Eur J Appl Physiol Occup Physiol* 70: 138–145, 1995.

FIGURE CAPTIONS

Figure 1

A. Motor unit discharge timings identified from surface EMG decomposition during an isometric sinusoidal contraction of the tibialis anterior muscle at a frequency of 0.5 (Hz) and a peak-to-peak amplitude of 5% MVC. **a.** Discharge timings of motor units of the same muscle during a contraction at the frequency of 1 Hz and same amplitude as in **A**. The black line in **A** and **a** represents the force during the sinusoidal force contractions in percentages of MVC. Each colour represents the discharge timings of an individual motor unit **B. and b.** The force signal and the motor unit discharge timings reported in **A-a** were low-pass filtered (2 Hz) in order to generate the smoothed discharge rate for each motor unit in **B. and b**. The smoothed motor unit spikes show a high degree of correlation with force. Moreover, it can be noted that they consistently anticipate the force for all the decomposed motor units. **C-c.** The individual motor unit discharge timings were summed in order to generate the cumulative spike trains (CST). After summation, the CST was filtered with a 2 Hz low-pass filter. The filtered CST and the force signal were cross-correlated in order to estimate the neuromechanical delay (NMD). Despite the force traces in the two cases have the same peak-to-peak amplitude, the greater frequency of force oscillation corresponds to a shorter NMD, that can be visually seen by comparing the epoch length between two green lines in **C and c**. **D-d.** and **E-e.** represent the same sinusoidal contraction in **A** and **a** but for the full duration of the task (2 min). **D-d**. A representative example of computation of the NMD as time lag of the peak of the cross-correlation function between the CST and the force signal for the full duration of the task. **E-e.** The cross-correlogram for the target sinusoid at 0.5 (Hz) and amplitude of 5% MVC (**E**) and the sine-wave at 1 (Hz) in (**e**) for the total length of the trial. The red dots are centred at the correlation peak (~0.8 correlation coefficient) and the position of the peak corresponds to the delay that is shown in **F** and **f.**

Figure 2

Estimates of the neuromechanical delay (NMD) as a function of the frequency of the force sinusoid for the first dorsal interosseous **(A)** and tibialis anterior muscle **(B)**. Each colour represents a different peak-to-peak amplitude of the sinusoidal force trajectory. The black lines indicate significant differences at $P < 0.05$.

Figure 3

The estimated neuromechanical delay (NMD) as a function of the maximum force derivative (maximum rate of change of force) for the first dorsal interosseous **(A)** and tibialis anterior muscle **(B)**. The force derivative depends on the product of the amplitude and frequency of the sinusoidal force trajectory and indicates the rate of force generation.

Figure 4

The average number of discharges per motor unit (total number of discharges across the detected motor unit population, divided by the number of detected motor units and by time) as a function of the maximum force derivative (maximum rate of change of force) for the first dorsal interosseous **(A)** and tibialis anterior muscle **(B)**.

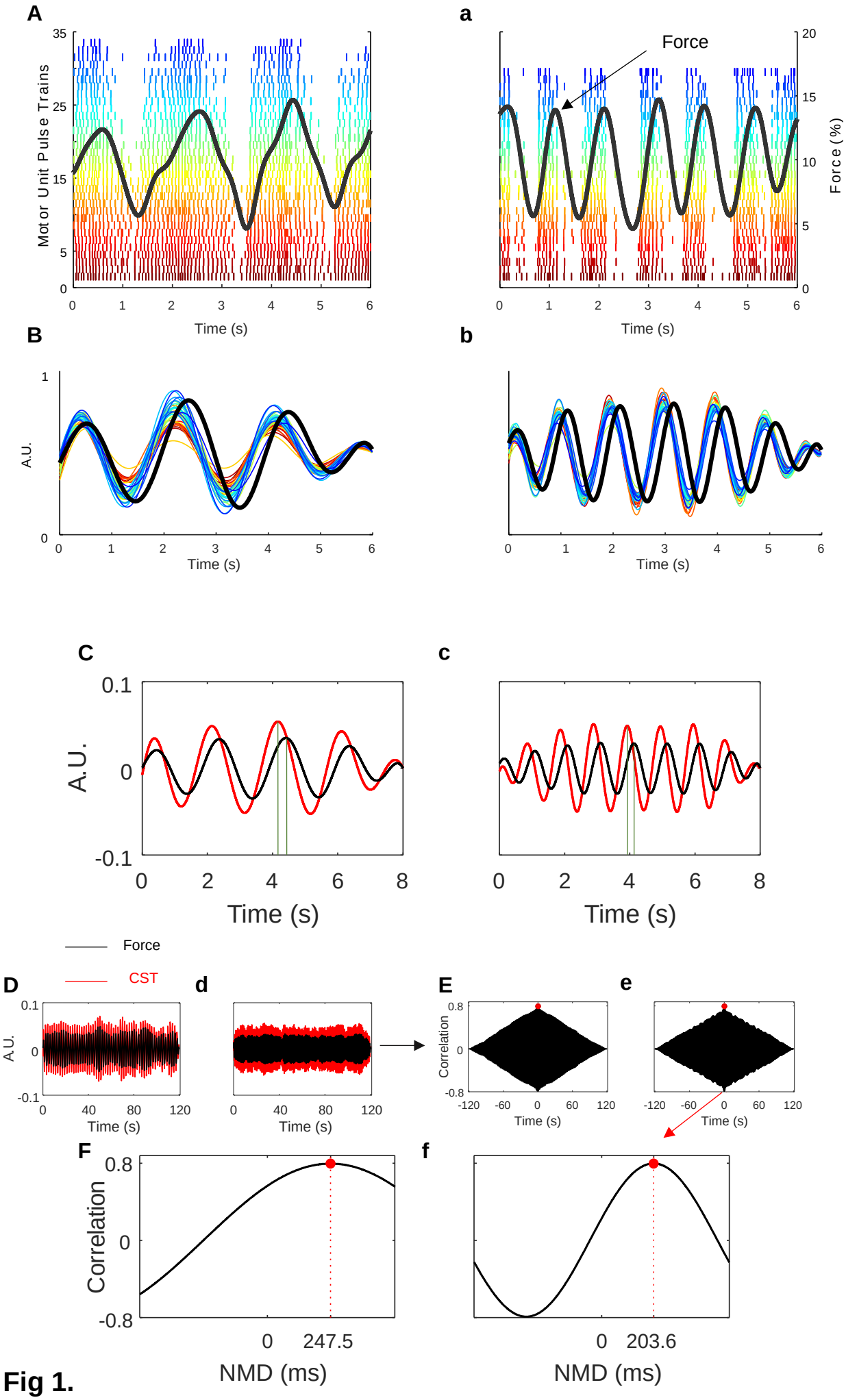

Fig 1.

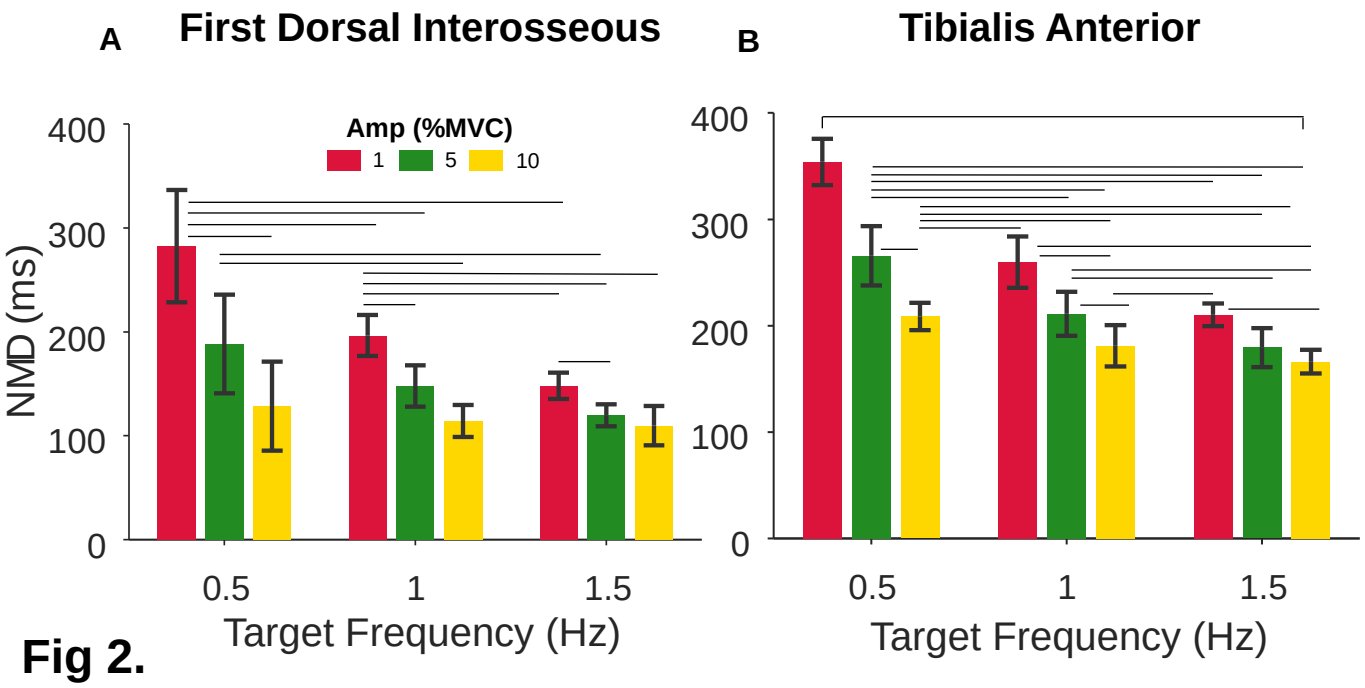

Fig 2.

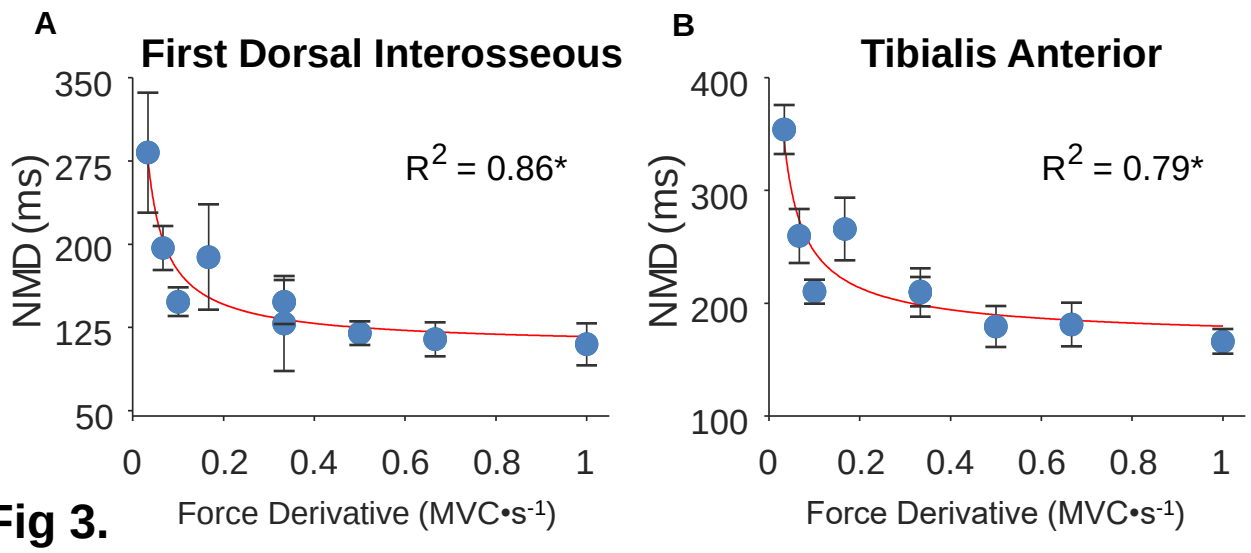

Fig 3.

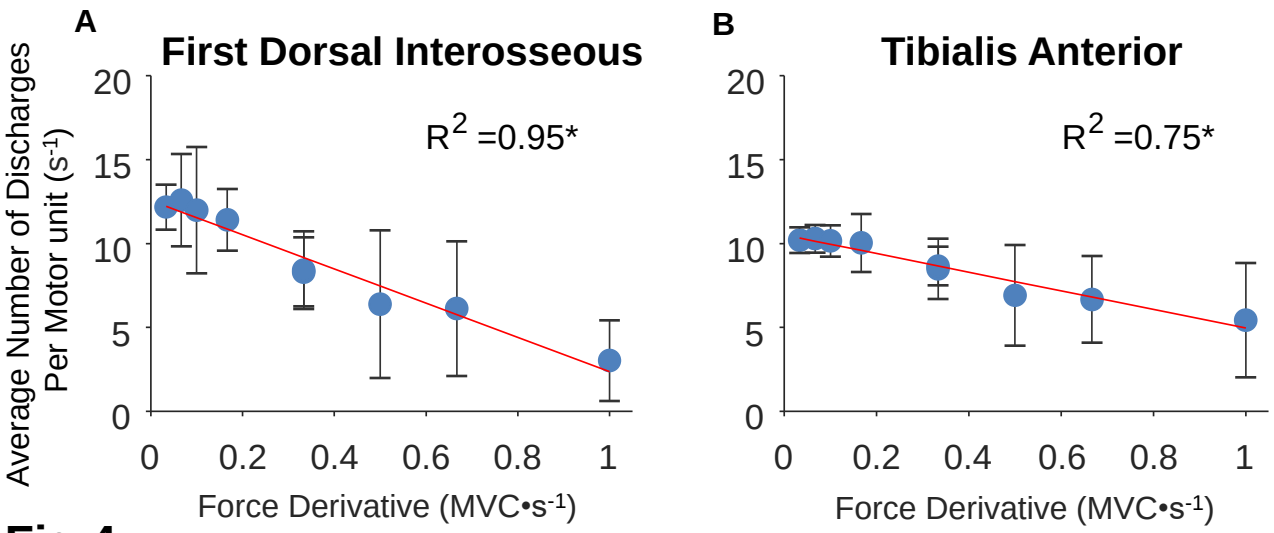

Fig 4.